Force-field Dependency of Leu-rich Helical Peptides Dimerization Energy in Lipid Bilayers. II. Limited Transferability of United-atom Simulation Parameters to Membrane-water Interfaces

Nishizawa M and Nishizawa K*

Teikyo University School of Medical Technology, Itabashi, Japan

Abstract

For molecular simulations of systems comprised of a lipid membrane and proteins, united-atom (UA) representation of aliphatic hydrocarbons can be a useful strategy to reduce the computational burden of all-atom (AA) representation. In a companion paper, however, we showed that transmembrane (TM) helical peptides of Leu-rich sequences and, to lesser degrees, of Ala- and Ile-rich helices show artifactually weak self-association propensities in phospholipid membranes under UA simulations. In the present paper, we show that this understabilization under UA models cannot be attributed to the inaccuracy in the dimerization energy of amino acid side chain analogues (SCAs). In fact, GROMOS 53A6 (Gr^{53a6}) force field (FF) yielded results similar to those with all-atom (AA) Charmm36 (Ch^{36AA}) FF in simpler systems, i.e., in the dimerization and solvation dynamics of amino acid SCAs in apolar solvents. The UA *vs.* AA discrepancy was not large for poly-Leu helices (either $(L)_7$ or $(L)_{21}$) dimerization in pure octane, but when more complex systems containing an octane slab/water or a phospholipid bilayer/water were used, the UA *vs.* AA discrepancy became pronounced, disfavoring the dimerization under Gr^{53a6}. Overall, our data demonstrate poor transferability of the UA FFs that are parameterized based on the amino acid SCAs dynamics with presumed transferability to phospholipid membrane/protein systems. Potential usefulness of our Lennard-Jones (LJ)-rescaling method, in which only the LJ terms between peptide and lipid atoms are modified, is discussed toward improved UA simulations of helical TM peptides embedded in phospholipid bilayers.

Introduction

Molecular dynamics (MD) simulations can be a useful tool to gain insights into the mechanisms for the folding processes and functions of membrane proteins at atomistic levels, which are of biomedical importance. A majority of the simulation-based studies in this area has recently been utilizing coarse-grained parameters [1-3]. Atomic details can only be addressed via all-atom (AA) or united atom (UA) models. However, while AA force fields (FFs), such as Charmm [4], Amber [5], general Amber [6] and SLipids [7], have been used in a growing number of studies, the computational burden seems to limit the system size and timescale of analyses. We have been studying on the dimerization dynamics of transmembrane (TM) helical peptides with simple sequences mainly using AA and UA models [8,9]. As UA models reduce the computational cost of a membrane protein embedded in explicit phospholipids to 30-20% of that with AA models, it seems worthwhile to improve the accuracy of UA force fields in peptides behavior in explicit phospholipid membranes [8,10].

In our companion paper [11], we reported that the UA models, GROMOS (Gr^{53a6}) and OPLS/Berger (OB) tend to show insufficient dimerization propensities of TM helical peptides with a variety of sequences. In particular, significant instability of the dimer of Leu-rich peptides, and to a lesser degrees, Ala- and Ile-rich peptides in the UA simulations was

observed in comparison with the AA simulations. To gain insights into the factors causative for this AA *vs.* UA discrepancy, this paper focuses on the energetics of the solvation and the self-association of select side chain analogues (SCAs) in apolar solvents. For such simpler systems, Gr^{53a6} unexpectedly showed a reasonable level of agreement to Ch^{36AA}, implying that, even if the UA parameters are adjusted guided by the experimental or AA-based SCA solvation/dimerization energies, poor transferability causes the inaccurate self-association energies for the helical peptides in phospholipid bilayers. Finally, to improve accuracy in the TM dimerization energy under Gr53a6, our attempt of reparameterization using a simple method (LJ-rescaling method) that downscales only the Lennard-Jones (LJ) terms between protein and lipid is discussed.

Methods

Molecular dynamics simulations were performed using the Gromacs package version 4.5.4 [12]. OPLS-all atom (AA) and Berger force fields and their combination were used as previously described [8]. Gr^{53a6} protein FF and the SPC water model were used as described in [11]. As Ch^{36AA}, the parameter file charmm36-jun2015.ff was used for both

peptides and lipids in combination with the TIPS3P water of the parameter set. For Ch^{36UA}, the parameters provided by Lee

et al. [13] was used in combination with the above TIPS3P water model. From the DOPC parameters of charmm36-jun2015.ff, we adopted the parameters for octane, and dibutyrylphosphatidylcholine (diC$_4$PC). We used the model peptides shown below:

L21:   Ac-LLLLLLLLLLLLLLLLLLLLL-amide
L7:   Ac-LLLLLLL-amide,

where Ac represents the acetyl group used for capping the N-terminus.

The following peptides analyzed in our companion paper [11] are discussed in the present paper as well.

A21:   Ac-AAAAAAAAAAAAAAAAAAAAA-amide
KL22:   Ac-KKG(L)$_{10}$W(L)$_{12}$KKA-amide and
        Ac-KKG(L)$_{10}$Y(L)$_{12}$KKA-amide
Ki23:   Ac-KKG(I)$_{23}$KKA-amide

For all simulations of this paper, the bond lengths of peptides and lipids were constrained using the LINCS algorithm [14], whereas those of water were constrained using the SETTLE algorithm [15].

Side chain analogues (SCAs) dimerization analysis

For SCAs for Asn and Ser, the dimerization $G^{PMF}(r)$ was obtained by unbiasing the umbrella sampling data (100 ns per window) with WHAM [16,17]. The umbrella sampling simulations were performed using the distance r between the two SCAs as the reaction coordinate. The windows for the umbrella sampling was set at r = 0.4−2.1 nm with a 0.1 nm interval. The effect of the entropic force due to the increase in the available phase space with the increase in r was removed from $G^{PMF}(r)$, and the obtained rdf profile, g(r), was assured to have an essentially flat curve for the range of r= ∼1−2 nm [18]. For Leu, Ile, Val and Phe, Ala, Met and Cys, five independent 200ns free runs were performed using the box of 4.5 nm and g(r) was obtained directly. The dimerization (binding) free energy ΔG^{dim} was estimated by integrating the g(r) based on the formula de Jong et al. [19], i.e., $\Delta G_{dim} = -RT \ln \left[\{(4\pi R_{max}^3)/(3v)\} \{\int_0^{rc} 4\pi r^2 * g(r) dr\} / \{\int_{rc}^{Rmax} 4\pi r^2 * g(r) dr\} \right]$, setting the rc value set at 1.0 nm. Here, $(4\pi R_{max}^3)/(3v)$ normalizes the volume used for the calculation of the denominator's integral and v is the standard volume 1.66 nm^3 equivalent to 1 mol/L [20].

Run parameters were similar to those used in our companion paper [11]. Briefly, the LJ interactions were treated with a shift function from 0.8 to 1.3 nm. The particle mesh Ewald method with a real-space cutoff of 1.4 nm and the minimal grid size of 0.12 nm was used to treat the long-range electrostatic energy. Integration time step of 3.3fs was used. To control the temperature at 323 K, the Berendsen thermostat was used. The isotropic pressure coupling at 1 bar with Berendsen barostat was used. For the measurements with octane as the solvent, a periodic cubic box of ∼4.5 nm on a side enclosing two SCA molecules/312 octane molecules was used.

Free energy perturbation (FEP)-based dimerization energy measurement

The umbrella sampling method used in our recent studies [11] was considered unsuitable to the dimerization analysis of the peptides embedded in the octane, octane/water or octane/dibutyrylphosphatidylcholine (diC$_4$PC)/water, as the termini of the two helices often bound to each other. So, for these systems, the dimerization energy was measured using the virtual bond/FEP method as follows. The center of mass (com) of the C$_\alpha$ atoms of the three amino acid residues located near the center of the peptide was considered dummy atom and named C1 and C2 for the two peptides, respectively. Then, a virtual-bond that links C1 to C2 was introduced and the FEP was performed in such a way that, to transform the system from the state A (the virtual bond length of 0.8 nm) to state B (2.0 nm), the coupling parameter λ was varied from 0 to 1 with an interval of 0.025 and a 100ns simulation was performed for each λ value. Five independent sets of analyses were performed and the standard error (S.E.) were obtained. The free energy difference between the two states (ΔG_{AB}) was derived from the gradient of the system's Hamiltonian (H) with respect to λ ($\partial H/\partial \lambda$ curve). To avoid the association between the peptide termini, another dummy atom (N1 and N2 for the two peptides, respectively) was introduced at the positions defined using the three C$_\alpha$ atoms located near the N-termini, and the angles C1-N1-N2 and N1-N2-C2 were restrained at the value of 90 degree using harmonic restraint of 1000 kJ/degree/mol. The dihedral angle describing peptide orientation was not restrained. To recover the free energy, the Bennett acceptance ratio (BAR) method [21] and the subsequent integration were performed using g_bar in Gromacs.

LJ interactions were treated with a shift function from 0.8 to 1.2 nm. The particle mesh Ewald method with a real-space cutoff of 1.21 nm and the minimal grid size of 0.12 nm was used. Integration time step of 3.3fs was used. Isotropic pressure coupling to 1 bar was performed using the Parrinello-Rahman method [22,23]. To couple the temperature at 323 K, the Nosé-Hoover-Langevin thermostat was used [24]. Typically, a periodic simulation boxes enclosing two L7/312 octane (a cubic box of ∼4.6 nm on a side), two L21/312 octane molecules and the two L21/246 octane/1300 water (with a ∼4.6 × 4.6 nm octane slab and the box height of ∼5.7 nm) were used.

Solvation energy analysis

The free energy perturbation (FEP) method employing the BAR analysis was used [21,25] for the solvation by octane and cyclohexane as in our recent report [8]. The intramolecular parameters were preserved to avoid in vacuo calculation. Coupling parameter λ was used for transforming the system from state A (λ = 0, coupled) to state B (λ = 1, decoupled). Equidistant λ-spacing with the spacing of 0.05 from 0 to 1 was used. For each λ value, 1 ns run was performed. From the $\partial H/\partial \lambda$ curve, ΔG_{AB} was derived. Ten independent sets were run and the standard error (S.E.) were obtained. The run parameters were similar to those used for the FEP-based dimerization analysis, but the time step of 2fs was used and the temperature was set at 298 K. For octane

solvation, a periodic cubic box (~4.5 nm on a side) enclosing the SCA and 312 octane was used. For the cyclohexane solvation, a periodic cubic box comprised of the SCA and 500 cyclohexane molecules was used.

Exposure analysis

The exposure index C_L represents the degree of exposure of each amino acid residue (or SCA) to solvent (lipids) atoms. C_L is defined as the mean number of lipid non-hydrogen atoms located within the cutoff distance (d_c) from at least one of the non-hydrogen atoms comprising the SC (or SCA). In the present study d_c was set at 4 Å. Similarly, we define C_{OP}, which is the mean number of the non-hydrogen atoms of the opposing peptide (C_{OP}) located within dc from at least one of the non-hydrogen SC atoms. Our in-house program that accounts for repetitive images due to the periodic boundary condition was used for the calculation.

LJ-rescaling method

This procedure modulates the strength (depth) of the LJ potential functions between protein atoms and lipid atoms, but preserves the parameters of the protein part and the lipid part of the FF, so as not to change the properties of pure bilayers nor of proteins in water of the original FFs [8]. The scaling factor k_{PL} is used to rescale the cross-term ε_{ij}, which is the depth of the well of the LJ energy between the atom i and j and normally defined as the geometric average of the ε assigned to each atom. So,

$$\varepsilon_{ij} = k_{PL}\sqrt{\varepsilon_{ii}\varepsilon_{jj}}$$

For each system, the uniform k_{PL} was used for both the backbone and the SC atoms of the peptides as well as for both the hydrocarbon chains and the headgroup atoms of the lipids. The run parameters were similar to those used for the SCA dimerization analysis, but, for the pressure coupling we used the isotropic coupling for the octane/diC4PC membrane system and the semi-isotropic coupling for the DOPC membrane. For the umbrella simulation-based dimerization energy measurements, the systems (peptides/DOPC/water and peptides/octane/diC$_4$PC/water) as well as the run parameters described in companion paper [11] were used.

Results

Solvation and dimerization of amino acid analogs in apolar solvents show concordance between UA and AA FFs: poor transferability to biologically relevant systems as the culprit

As our companion paper showed, the dimerization energy of the Lys-flanked poly-Leu peptide (KL22) in the DOPC bilayer was only −1.55 kJ/mol under Gr[53a6], showing much weak dimerization propensity compared to −7.46 kJ/mol under Ch[36AA] (#1 and #6 of Table 1 of [11]). A similar difference was observed for the L21/DOPC systems (#8 and #9 in [11]). The difference was mitigated but still substantial when, instead of the DOPC bilayer, a slab of octane/dibutyrylphosphatidylcholine (diC$_4$PC) was used (#2 vs. #7 and #10 vs. #11 of [11]). Of note, the octane/diC$_4$PC is a mimetic of phospholipid bilayers and was found useful to obtain quick convergence in computation, but it has not fully been characterized in the peptide solvation by lipids in comparison with phospholipid bilayers.

	Ch[36AA]	Ch[36UA]	Gr[53a6]		OPLS-Berger		experiment[1)]
	octane	octane	octane	CHX	octane	CHX	CHX
isobutane (Leu)	-9.2 ± 0.1	-10.8 ± 0.1	-10.4 ± 0.1	-11.0 ± 0.1	-11.8±0.1	-11.9 ± 0.2	-10.9
butane (Ile)	-10.2 ± 0.1	-12.3 ± 0.1	-11.4 ± 0.1	-12.4 ± 0.1	-12.0±0.1	-12.2 ± 0.1	-11.4
propane (Val)	-7.0 ± 0.1	-8.3 ± 0.1	-7.9 ± 0.1	-8.6 ± 0.1	-8.1±0.1	-8.5 ± 0.1	-8.5
toluene (Phe)	-19.9 ± 0.1	-21.8 ± 0.1	-19.9 ± 0.1	-20.2 ± 0.1	-19.3±0.1	-20.0 ± 0.1	-17.5
acetamide (Asn)	-10.7 ± 0.1	-11.1 ± 0.1	-11.7 ± 0.1	-12.0 ± 0.1	-12.6 ± 0.1	-13.3 ± 0.1	-12.6
methanol (Ser)	-3.4 ± 0.1	-3.3 ± 0.1	-4.4 ± 0.1	-4.4 ± 0.1	-3.7 ± 0.1	-4.0 ± 0.1	-6.9

[1)] ref [26]

Table 1: Free energy (in kJ/mol) of solvation in octane and cyclohexane (CHX) for select amino acid SCAs computed with four different parameter sets. The average of ten trials is shown along with S.E. of the mean.

In theory, the stronger (i.e., energetically favorable) SCA solvation by lipids leads to the more stable monomeric state, causing the destabilization of the dimeric state of TM helices. So, we addressed the question whether the between-FF discrepancy in the Leu-rich helices dynamics is tractable to the incomplete parameterization of the UA FFs in the SCA dynamics. To this end, we computed the solvation energies of

the SCAs by the apolar solvents (octane and, for Gr[53a6] and OB, cyclohexane) under each FF (Table 1). Relatively strong solvation with the UA FFs and weak solvation with Ch[36AA] were observed for the aliphatic SCAs, but the differences were small (Table 1). For example, the octane solvation energy for the Leu SCA was −9.2 kJ/mol with Ch[36AA] and −10.4 kJ/mol with Gr[53a6]. While this Gr[53a6] > Ch[36AA]

difference in the (unsigned) energy might have contributed to weakening the TM dimerization under the UA FFs, this difference seemed too small to explain the difference in the TM dimerization. At least, the exposure analysis showed that, except for two or three residues located in the peptide-peptide interface, no Leu residues underwent significant changes (>3) in the C_L (i.e., the mean number of lipid non-hydrogen atoms located within 4 Å from at least one of the non-hydrogen atoms comprising the SC) between the dimeric and monomeric states in the DOPC bilayer. Moreover, even for those Leu residues whose C_L drop was >3 upon the dimerization, the decrease was compensated by the nearly equal number C_{OP} of the atoms, located within 4 Å, of the opposing helical peptide upon dimerization. These findings argued against the view that the wide between-FF discrepancy in the TM dimerization was caused by the inaccurate parameterization based on the SCAs dynamics. Moreover, for the SCAs of Leu, Ile and Val, the solvation by octane was favored in the order of $Ch^{36UA} > Gr^{53a6} > Ch^{36AA}$ (Table 1), which does not explain the order of $Ch^{36AA} > Ch^{36UA} > Gr^{53a6}$ in the stability of KL22 dimerization (#1 , #3 and #6 as well as #2, #4 and #7 in [11]). Collectively, the differences in the solvation data (Table 1) did not appear to explain the observed FF-dependency of the TM dimerization data.

As the solvation data are of value from a general perspective, we carried out an additional analysis on SCAs of Ser, Asn and Phe following the related studies [17,20]. Broadly, the FF-dependent difference was small for these SCAs, the difference ranging ± 2 kJ/mol.

Setting aside the between-FF differences, Table 1 shows overall similarity between the in-cyclohexane and in-octane data for each FF, suggesting that the transferability of the UA and AA parameters between cyclohexane and linear alkanes is fairly good.

Next, we addressed the question whether the parameter improvement based on the dimerization energies of the SCAs in apolar solvents is useful for UA simulations of the TM dimerization. To this end, the dimerization energies for the SCAs in apolar solvents and vacuum were computed (Table 2). The in-octane dimerization propensity of the SCA for Leu showed a $Ch^{36AA}>Gr^{53a6}>OB$ difference, which was consistent with the order seen for the dimerization propensity of the model peptides we recently used, i.e., $(AALALAA)_3$, L21 and KL22 [11]. However, here again, the dimerization energies of the aliphatic amino acids showed rather small between-FF differences (Table 2), which could not explain the wide FF-dependency in the TM dimerization. For example, for the Leu SCA dimerization, Gr^{53a6} and Ch^{36AA} showed only a 0.08 kJ/mol difference, which does not explain the >5 kJ/mol difference in the L21 dimerization in the DOPC bilayer, that is, -0.24 kJ/mol (with Gr^{53a6}) and -6.12 kJ/mol (with Ch^{36AA}) [11], which reinforces the view of poor transferability in the light of the above consideration on C_L. Overall, these findings implicate the limited transferability of the UA parameters, rather than inadequate optimization of the parameters based on the simpler systems, as the cause for the insufficient TM dimerization energy for the Leu-rich peptides.

For all SCAs tested in Table 2, the results were in agreement with the study by de Jong et al. [20], which used decane as the solvent.

Dimerization	Ch^{36}		Gr^{53a6}		OPLS-Berger
	octane	vacuum	octane	vacuum	octane
toluene (Phe)	-1.18 ± 0.07	-2.10 ± 0.01	-1.22 ± 0.03	-2.02 ± 0.03	-1.23 ± 0.05
isobutane (Leu)	-1.25 ± 0.04	-1.52 ± 0.01	-1.17 ± 0.02	-1.60 ± 0.02	-1.10 ± 0.04
butane (Ile)	-1.31 ± 0.05	-1.57 ± 0.02	-1.24 ± 0.03	-1.59 ± 0.04	-1.19 ± 0.01
propane (Val)	-1.26 ± 0.04	-1.44 ± 0.01	-1.16 ± 0.04	-1.46 ± 0.01	-1.22 ± 0.03
methane (Ala)	-1.31 ± 0.07	-1.29 ± 0.01	-1.29 ± 0.02	-1.27 ± 0.02	n.d.
methyl-ethylsulfide (Met)	-1.17 ± 0.06	-1.81 ± 0.02	-1.33 ± 0.04	-2.01 ± 0.02	n.d.
methanethiol (Cys)	-1.30 ± 0.02	-1.50 ± 0.02	-1.45 ± 0.03	-1.50 ± 0.02	n.d.

[1] n.d. = not determined

Table 2: Free energy for dimerization in octane and in vacuum[1].

Overall, these results argue that the UA parameters for Leu have limited transferability between the SCA/apolar solvent systems and the TM/phospholipid bilayer systems. The results on the Ala SCA also showed limited transferability. For A21 the TM dimerization in the octane/diC$_4$PC/water showed a difference between the FFs (-1.95 with Gr^{53a6} and -3.86 kJ/mol with Ch^{36AA}) [11], but this cannot be explained by the SCA dimerization dynamics that showed good agreement between Gr^{53a6} and Ch^{36AA} (Table 2).

Parameter transferability worsens with the systems containing lipid-water interface

To gain further insights into the step at which the limited transferability of Gr^{53a6} starts to manifest, the self-dimerization energy was measured for the systems with different degrees of biological reality: L7/octane, L21/octane, and L21/octane/water. Table 3 show the results in comparison with L21/octane/diC$_4$PC/water and L21/DOPC/water [11]. Intriguingly, as the system became progressively complex and physiologically relevant, the parameter transferability appeared to worsen. That is, the Gr^{53a6} - Ch^{36AA} discrepancy was seen for the octane water system, but it increased as the interface becomes more realistic as shown for the octane/diC$_4$PC/water system and further the DOPC/water system. Thus, the comparison with the Ch^{36AA} results suggest that a challenge in the UA model simulations is difficulty to faithfully represent lipid-water interfaces. The AA-UA discrepancy was more significant for phospholipid bilayer-containing systems likely because of difficulty in representing realistic lipid headgroups-peptide interaction, although we cannot rule out the possible difficulty in representing the Leu interaction with the acyl chains of phospholipids that by and large orient along the membrane normal, unlike octane.

	Gr^{53a6} (kJ/mol)	Ch^{36AA} (kJ/mol)
L7/octane (no-water)	-4.5 ± 0.2	-3.3 ± 0.1
L21/octane (no-water)	-4.3 ± 0.4	-4.3 ± 0.3
L21/octane/water	-3.0 ± 0.2	-3.7 ± 0.7
L21/octane/diC$_4$PC/water[1)	-0.3 ± 0.4	-2.4 ± 0.6
L21/DOPC/water[1)	-0.2 ± 0.8	-6.1 ± 2.0

[1) Results based on the potential of mean force (PMF) analysis that we recently reported [11].

Table 3: FEP computation of energy (± SE) for self-dimerization of L7 and L21.

Application of LJ–rescaling method to UA FFs guided by CHARMM FF improves the TM interaction energetics

Disease-related single-pass TMs relevant for cellular signaling showed a composition biased toward V, L, and I [11]; it is most likely that branched-chain amino acids (L, I, and V) account for about a half of the residues of such TMs.

Given the limited transferability of the UA parameters discussed above, reparameterization of Gr53a6 parameters was conducted using the Ch^{36AA} –based TM dimerization data as the reference. We here present a few examples of the application of our LJ-rescaling method [8]. Of note, this method preserves the parameters of the lipids part and the protein part of the original FFs, but changes only the LJ terms between lipid and protein atoms (cross-terms). Thus, specific protein-protein as well as specific lipid-lipid interactions remain unchanged from the original Gr^{53a6}. The interaction of amino acids with water was also unchanged from the original Gr^{53a6}. As the first example, the LJ terms between Leu and lipids of Gr^{53a6} were rescaled such as to render the L21 dimerization in the octane/diC$_4$PC/water close to that with Ch^{36AA} (Figure 1A). Although our trials with k_{PL} = 0.85, 0.9 and 0.92 were all found too drastic, the octane/diC$_4$PC/water system may be useful as it allows rapid convergence. (The estimated dimerization energy is listed in the legend for Figure 1.) The LJ-rescaling procedure was also used for Ile21 dimerization in the DOPC/water system used in our companion paper [9,11]. The LJ-rescaled Gr^{53a6} with k_{PL} = 0.95 showed improved accuracy in dimerization with respect to the Ch^{36AA} data (Figure 1B). Although we have not tested, the LJ-rescaling may be extended in an amino acid residue position-specific manner that, for example, employs distinct k_{PL} values for the residues near headgroups and for those close to hydrophobic core on the membrane. Such a rescaling methods may benefit UA simulation analyses of TM helices dynamics.

Conclusion

In our companion paper we showed that the dimeric state of TM poly-Leu helical peptides in a DOPC bilayer under GROMOS 53A6 (Gr^{53a6}) FF was unstable in contrast to the experiment as well as all-atom CHARMM36 (Ch^{36AA}) simulation, while both of the latter showed dimerization propensity. A CHARMM-based united-atom FF (Ch^{36UA}) showed an intermediate degree of dimerization propensity between Ch^{36AA} and Gr^{53a6}. A small but significant Ch^{36AA}>Gr^{53a6} difference was observed for the dimerization propensity of a poly-Ala TM peptide. The poly-Ile helical peptides also showed some AA-UA discrepancy in DOPC bilayer (Figure 1). As we showed in this study, the deficiency in the Leu- and the Ala-rich peptides dimerization energies under the UA FFs could not be ascribed to the artifactually favored solvation of the amino acid residues by apolar solvents. Together with our recent report on (AALALAA)$_3$ peptide [8], these results suggest that dimerization of Leu residues (and Ala residues) located near the phospholipid headgroup is prone to inaccuracy due to limited parameter transferability. Thus, conventional bottom-up parameterization approaches for UA FFs based on the SCAs solvation energies can lead to erroneous molecular behaviors upon applications in protein/phospholipid membrane systems.

Given the relatively accurate and consistent TM dimerization under Ch^{36AA}, we suggest reparameterization directly focusing on the TM association energies under an AA FF, such as Ch^{36AA} as a reference. We also showed that, by applying the LJ-rescaling method to Gr^{53a6}, the accuracy of the UA FF in TM dimerization can be improved.
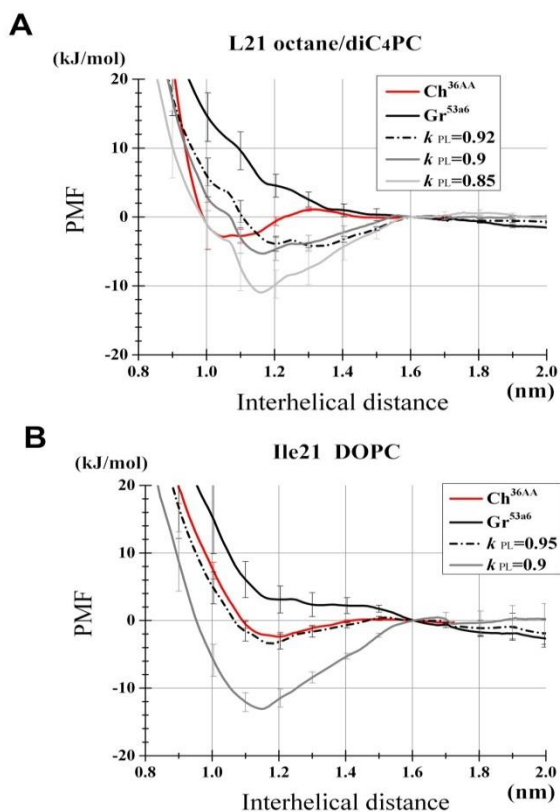

Figure 1: Potential of mean force (PMF) profiles of the TM helices dimerization under the original FFs and the Gr^{53a6} FF reparameterized using our LJ-rescaling methods. (A) Rescaling of Leu-lipid LJ terms of Gr^{53a6} guided by the Ch^{36AA}-based L21 dimerization energy in the L21/octane/diC4PC systems. Rescaling schemes with k_{PL} = 0.85, 0.9 and 0.92 were examined. Error bars represent SEs from five independent umbrella analysis sets. The values relative to the average of the values at r = 1.6 nm are plotted. The dimerization energy ΔG^{dim} for each scheme derived as described in our companion paper [11] was; Ch^{36AA}, −2.11; Gr^{53a6}, −0.32; Gr^{53a6} (k_{PL} 0.85), −4.85; Gr53a6 (k_{PL} 0.9), −2.88; and Gr53a6 (k_{PL} 0.92), −2.52 kJ/mol. Of note, the measurements with Ch^{36AA} and Gr^{53a6} were based on the data used in [11] but recalculated after some additional simulations. (B) Rescaling of the Gr^{53a6} Ile-lipid LJ terms guided by Ile21 dimerization in the Ile21/DOPC/water system under the Ch^{36AA}. ΔG^{dim} based on the method we described in [11] was; $Ch3^{6AA}$, −1.74; Gr^{53a6}, 0.23; Gr^{53a6} (k_{PL} 0.9), −5.8; and Gr^{53a6} (k_{PL} 0.95), −1.75 kJ/mol. The measurements with Ch^{36AA} and Gr^{53a6} were based on the data used in [9] but recalculated after extended simulations.

In this study, the AA *vs.* UA discrepancy increased as the systems became more complex and physiologically relevant. However, it remains to be answered why Leu and Ala suffer from poor transferability, when poly-Ile and poly-

Val showed results fairly consistent with Ch^{36AA} at last in the octane/diC4PC system [11]. Representation of interaction between phospholipid headgroups and Leu (or Ala) on TM helices may be specifically inaccurate in UA representation. Further analyses are necessary to address this issue. In any case, our results suggest that care should be taken to the amino acid-lipid headgroup interactions. Considering our recent finding that the raft-like phospholipid bilayers stabilize the dimeric state of poly-Ile helices and this effect is mainly mediated by the electrostatic energy between the peptides and phospholipid headgroups [9], it seems possible that even in the case with aliphatic amino acids-rich peptides, the electrostatic interactions between peptide backbone and lipid headgroups become a key factor requiring accurate representation for TM-TM association analyses. Besides, because many TM helical peptides harbors large residues such as Trp and Lys near the phospholipid headgroup and because such bulky SCs are likely to be influential in solvation/dimerization, simulations of TM interaction would require careful description of such moieties.

Parameters of current biomolecular FFs were usually tuned to give accurate fits to energy profiles based on quantum computation, as well as to reproduce enthalpies of vaporization and densities for pure liquids [27]. Partition coefficients and solvation of SCAs by apolar solvents were computed for several FFs by several authors [28-30], but parameterization prioritizing partition/solvation appears difficult due to requirements in reproducing fundamental properties of proteins and lipids. However, for the membrane protein analyses, precise adjustment of UA parameters in terms of partition and solvation has a limited importance because deficient transferability at another level of complexity complicates. These point to importance of adjustment in setting close to the system of interest.

Tieleman and coworkers have discussed the challenges in using a protein FF optimized for aqueous environments in combination with a FF prepared for lipid membranes [10]. Our studies suggest that even well-studied UA FFs for both lipids and proteins can exhibit limited transferability especially in protein/lipid interaction near lipid headgroups. AA FFs are likely to have significantly better suitability for analyses of TM peptide interaction than UA FFs. When combining UA lipids with protein FFs, in some cases it is advised to adjust the parameters based on TM-TM interaction directly, rather than based on SCA interactions. Although our LJ-rescaling shown in Figure 1 used the invariant rescaling factor (k_{PL}) over all amino acid residues of the peptides, further analyses to evaluate the inaccuracy of the Leu-lipids interaction energy taking into account of the SC location within the peptide (e.g., the termini or central segments) would be helpful. Finally, this study used only the fixed-charge (additive) models, leaving use of polarizable FFs to future studies. Use of polarizable FFs may serve for membrane simulations or, as a reference, for reparameterization of UA FFs.

Competing Interests

Nishizawa M, Nishizawa K (2018) Force-field Dependency of Leu-rich Helical Peptides Dimerization Energy in Lipid Bilayers. II. Limited Transferability of United-atom Simulation Parameters to Membrane-water Interfaces. Ann Biomed Res 1: 113.

The authors declare that they have no competing interests.

References

1. Izvekov S, Voth GA (2006) Multiscale coarse-graining of mixed phospholipid/cholesterol bilayers. J Chem Theory Comput 2(3): 637-648.

2. Marrink SJ, De Vries AH, Tieleman DP (2009) Lipids on the move: Simulations of membrane pores, domains, stalks and curves. Biochimica et Biophysica Acta (BBA)-Biomembranes 1788(1): 149-168.

3. Pluhackova K, Böckmann RA (2015) Biomembranes in atomistic and coarse-grained simulations. J Phys Condens Matter 27(32): 323103.

4. Klauda JB, Venable RM, Freites JA, et al. (2010) Update of the CHARMM all-atom additive force field for lipids: Validation on six lipid types. J Phys Chem B 114(23): 7830-7843.

5. Skjevik AA, Madej BD, Walker RC, Teigen K (2012) LIPID11: A modular framework for lipid simulations using amber. J Phys Chem B 116(36): 11124-11136.

6. Dickson CJ, Rosso L, Betz RM, et al. (2012) GAFFlipid: A general amber force field for the accurate molecular dynamics simulation of phospholipid. Soft Matter 8(37): 9617-9627.

7. Jämbeck JPM, Lyubartsev AP. (2012) Derivation and systematic validation of a refined all-atom force field for phosphatidylcholine lipids. J Phys Chem B 116(10): 3164-3179.

8. Nishizawa M, Nishizawa K (2016) Free energy of helical transmembrane peptide dimerization in OPLS-AA/Berger force field simulations: Inaccuracy and implications for partner-specific Lennard-Jones parameters between peptides and lipids. Molecular Simulation 42(11): 916-926.

9. Nishizawa M, Nishizawa K (2018) Sequence-nonspecific stabilization of transmembrane helical peptide dimer in lipid raft-like bilayers in atomistic simulations. I. Dimerization free energy and impact of lipid-peptide potential energy. Ann Biomed Res 1(1): 105.

10. Tieleman DP, MacCallum JL, Ash WL, et al. (2006) Membrane protein simulations with a united-atom lipid and all-atom protein model: Lipid–protein interactions, side chain transfer free energies and model proteins. J Phys Condens Matter 18(28): S1221 -1234.

11. Nishizawa M, Nishizawa K (2018) Force-field dependency of Leu-rich helical peptides dimerization energy in lipid bilayers. I. United-atom simulations show discrepancy from experiments and all-atom imulations. Ann Biomed Res 1(2): 112.

12. Pronk S, Páll S, Schulz R, et al. (2013) GROMACS 4.5: A high-throughput and highly parallel open source molecular simulation toolkit. Bioinformatics 29(7): 845-854.

13. Lee S, Tran A, Allsopp M, et al. (2014) CHARMM36 united atom chain model for lipids and surfactants. J Phys Chem B 118(2): 547-556.

14. Hess B, Bekker H, Berendsen HJC, et al. (1997) LINCS: A linear constraint solver for molecular simulations. J Comput Chem 18: 1463-1472.

15. Miyamoto S, Kollman PA (1992) SETTLE: An analytical version of the SHAKE and RATTLE algorithm for rigid water models. J Comput Chem 13: 952-962.

16. Kumar S, Rosenberg JM, Bouzida D, et al. (1992) The weighted histogram analysis method for free-energy calculations on biomolecules. I. The method. J Comput Chem 13: 1011-1021.

17. Mirjalili V, Feig M (2015) Interactions of amino acid side-chain analogs within membrane environments. J Phys Chem B 119(7): 2877-2885.

18. Hess B, Holm C, van der Vegt N (2006) Osmotic coefficients of atomistic NaCl (aq) force fields. J Chem Phys 124(16): 164509.

19. De Jong DH, Schäfer LV, De Vries AH, et al. (2011) Determining equilibrium constants for dimerization reactions from molecular dynamics simulations. J Comput Chem 32(9): 1919-1928.

20. De Jong DH, Periole X, Marrink SJ (2012) Dimerization of amino acid side chains: Lessons from the comparison of different force fields. J Chem Theory Comput 8(3): 1003-1014.

21. Bennett CH (1976) Efficient estimation of free energy differences from Monte Carlo data. J Comput Phys 22(2): 245-268.

22. Parrinello M, Rahman A (1981) Polymorphic transitions in single crystals: a new molecular dynamics method. J Appl Phys 52(12): 7182-7190.

23. Parrinello M, Rahman A (1982) Strain fluctuations and elastic constants. J Chem Phys 76(5): 2662-2666.

24. Nosé S (1986) An extension of the canonical ensemble molecular dynamics method. J Molecular Phys 57(1): 187-191.

25. Shirts MR, Pande VS (2005) Comparison of efficiency and bias of free energies computed by exponential averaging, the Bennett acceptance ratio, and thermodynamic integration. J Chem Phys 122(14): 144107.

26. Radzicka A, Wolfenden R (1988) Comparing the polarities of the amino acids: Side-chain distribution coefficients between the vapor phase, cyclohexane, 1-octanol, and neutral aqueous solution. Biochemistry 27: 1664-1670.

27. Shirts MR, Pande VS (2005) Solvation free energies of amino acid side chain analogs for common molecular mechanics water models. J Chem Phys 122(13): 134508.

28. Oostenbrink C, Villa A, Mark AE, et al. (2004) A biomolecular force field based on the free enthalpy of hydration and solvation: The GROMOS force-field parameter sets 53A5 and 53A6. J Comput Chem 25(13): 1656-1676.

29. Sapay N, Tieleman DP (2011) Combination of the CHARMM27 force field with united-atom lipid force fields. J Comput Chem 32(7): 1400-1410.

30. Cordomí A, Caltabiano G, Pardo L (2012) Membrane protein simulations using AMBER force field and berger lipid parameters. J Chem Theory Comput 8(3): 948-958.

*Corresponding author: Kazuhisa Nishizawa, MD, PhD, Department of Clinical Laboratory Science, Teikyo University School of Medical Technology, 2 Kaga, Itabashi, Tokyo, 173-8605 Japan, Tel: +81-3-3964-1211; Email: kazunet@med.teikyo-u.ac.jp